Available online at www.sciencedirect.com
SCIENCE DIRECT®
Intermetallics 11 (2003) 1293–1299
Intermetallics
www.elsevier.com/locate/intermet

Driving forces for crystal nucleation in Fe–B liquid and amorphous alloys

M. Palumbo[a], G. Cacciamani[b], E. Bosco[a], M. Baricco[a,*]

[a]Dip. Chimica I.F.M. and INFM/INSTM, Università di Torino, via Giuria 9, 10125 Torino, Italy
[b]Dip. Chimica e Chimica Industriale, Università di Genova, via Dodecanneso 31, 16146 Genova, Italy

Abstract

The Fe–B system has been reassessed in order to model metastable and amorphous phases. An excess specific heat term has been added to describe Gibbs free energy of the liquid phase on undercooling and glass transition has been considered as a second-order transition. In addition, a recently proposed description of pure Fe lattice stabilities has been used for this optimisation. Stable and metastable phase diagrams have been calculated, as well as thermodynamic properties, which turn out in agreement with experimental data. Thermodynamic driving forces for crystal nucleation have also been evaluated for liquid and amorphous phases. According to experimental findings, it was found that the first nucleating phase is b.c.c. Fe for B-poor amorphous alloys. However, for B-rich compositions, a competition between Fe_2B and Fe_3B nucleation has been evidenced. A full explanation of the crystallisation process requires the evaluation of interfacial energies.

Keywords: B. Glasses; Metallic; Thermal stability; C. Casting (including segregation); E. Phase diagram prediction (including CALPHAD)

1. Introduction

Nanocrystalline materials have been widely studied in recent years because they show attractive technological properties. These materials are often produced from an amorphous matrix by controlled crystallisation, which can be described by a nucleation and growth mechanism [1,2].

Critical parameters necessary in the classical nucleation and growth theory are the interfacial energy σ between the old phase and the new one, the diffusion coefficient D and the driving forces for nucleation ΔG, that is the Gibbs free energy difference between the old and the new phase. A number of models are available for a theoretical estimation of interfacial energies, which can predict its variation with temperature and composition [3–5]. However, measurements of these quantities are extremely sensitive to experimental settings and modelling is not yet well assessed. Diffusivity can instead be determined directly from tracer experiments or indirectly by studying the kinetics of crystal growth. Data are available for many amorphous alloys [6]. The direct simulation of diffusion in amorphous phases, generally by Molecular Dynamics or Monte Carlo methods, is currently far a delicate task owing to present-day limitations in computing capabilities. Finally, driving forces can be determined from the knowledge of Gibbs energy of the phases involved, which can be calculated from thermodynamic models [7] or using the CALPHAD method.

In this paper, we have focused our attention on the Fe–B system, which is of interest in several fields of materials engineering. This system shows a significant glass forming ability (GFA) for compositions close to the Fe-rich eutectic [8] and it is often used as a model system for the understanding of glass formation and crystallisation in metallic materials.

Several critical evaluations of this system have been performed by many authors [9–15], but they considered only stable phases. In order to calculate driving forces for crystallisation, a thermodynamic analysis of the system by means of the CALPHAD approach is necessary, including metastable and amorphous phases.

In the following we present a new assessment of the Fe–B system. Modelling for binary amorphous and undercooled liquid phases has been applied as in previous assessments [16–18]. In the present optimisation we have used new lattice stabilities (reported in Ref.

* Corresponding author. Tel.: +39-011-670-7569; fax: +39-011-670-7855.
E-mail address: marcello.baricco@unito.it (M. Baricco).

0966-9795/$ - see front matter © 2003 Elsevier Ltd. All rights reserved.
doi:10.1016/S0966-9795(03)00171-7

[19]) to describe thermodynamic properties for pure Fe. From assessed parameters, driving forces for crystal nucleation from liquid and amorphous phases have been calculated and the crystallisation mechanisms have been examined.

2. Modelling

Depending on concentration, the transition from a metastable amorphous phase into equilibrium crystalline phases can occur through following reactions [8]:

- Polymorphous crystallisation, i.e., a partitionless growth of the new crystalline phase with a different crystal structure but with the same composition as the amorphous matrix. This reaction can only occur in a concentration range near the pure elements or compounds and may eventually lead to a supersaturated solid solution, which undergoes further precipitation until the stable equilibrium is reached.
- Eutectic crystallisation, i.e., the cooperative growth of two crystalline phases by a discontinuous reaction. In this kind of process there is no concentration difference across the reaction front, but short-range diffusion takes place parallel to the reaction front and the two components have to separate into two different phases.
- Primary crystallisation, i.e. the formation of a new crystalline phase with a composition different from the amorphous matrix. During this reaction, a diffusion gradient forms and the matrix enriches in one of the components until a metastable equilibrium is reached. The reaction can then proceed by one of the previous described mechanisms.

In the first process, the calculation of driving forces is straightforward, implying the calculation of a simple difference between the Gibbs energies of the involved phases. For a primary or eutectic crystallisation the driving force depends on the composition of the nucleus that will firstly form.

Christian [20] has shown that, for a binary AB system, these quantities can be calculated from Gibbs free energy-composition curves at a given temperature. The driving force is maximum when the tangents to the crystalline and amorphous Gibbs energy curves are parallel, that is in mathematical terms when

$$\left(\frac{\partial G^{\mathrm{cryst}}}{\partial X}\right)_{X_n} = \left(\frac{\partial G^{\mathrm{am}}}{\partial X}\right)_{X_0} \tag{1}$$

where X_n is the composition of the most probable nucleus (for which ΔG is maximum), X_0 is the composition of the amorphous matrix, G^{cryst} and G^{am} are the Gibbs free energies of crystal and amorphous matrix respectively. Then, driving force for nucleation of crystals is given from:

$$\Delta G = \mu_{\mathrm{A}}^{\mathrm{cryst}} - \mu_{\mathrm{A}}^{\mathrm{am}} \tag{2}$$

where $\mu_{\mathrm{A}}^{\mathrm{cryst}}$ and $\mu_{\mathrm{A}}^{\mathrm{am}}$ are chemical potentials of component A for crystalline and amorphous phases.

If amorphous and crystalline phases can be described by simple models, an analytical expression may be obtained for driving forces and for the composition of the nucleus according to Eqs. (1) and (2). Thompson and Spaepen [7] have shown that, if the amorphous phase is described by a regular solution model and the nucleation of an almost pure element is considered, the following approximate formula may be used:

$$\Delta G = (T_{\mathrm{l}} - T)\left(\Delta S_{\mathrm{melt}}^{\mathrm{A}} - R\ln X_0\right) \tag{3}$$

where $\Delta S_{\mathrm{melt}}^{\mathrm{A}}$ is the entropy of melting of pure A component, T_{l} is the liquidus temperature at X_0 composition according to the phase diagram and R is the gas constant.

However the regular solution model is often inadequate to describe real systems. In addition, liquid-amorphous behaviour requires a different treatment and complex models must be adopted following the CALPHAD approach. Metastable compounds can also form during the crystallisation process and a proper description of their thermodynamic functions is also needed. So, in order to calculate the driving forces for crystallisation in the Fe–B system we have improved previous assessments introducing the modelling of metastable phases and considering new experimental data for these phases.

Fe–B binary system consists of six equilibrium phases: liquid, three terminal solid solutions, b.c.c. Fe (αFe and δFe), f.c.c. Fe (γFe) and rhombohedral B (βB), and two intermediate compounds Fe_2B and FeB. Fe_3B is generally considered a metastable phase. It is one of the crystallisation products, so it was included in our CALPHAD optimisation.

The SGTE description of lattice stabilities is the most widely accepted because it is simple and in good agreement with experimental data. However, the SGTE database uses mathematical polynomials to interpolate thermodynamic functions of pure elements. A more physical description is desirable, containing parameters of physical significance. A step in this direction has been carried out by Chen and Sundman [19], who used some models to describe the thermodynamic functions of pure Fe. In particular, they have used the so-called "generalized two-state model" [21] to describe the liquid and amorphous phases, which have been considered as a single phase in which the atoms can be in either the

"amorphous-like" or "liquid-like" state. According to this model, Gibbs free energy for liquid–amorphous pure Fe ($^0G_{Fe}^{liq-am}$) is given by

$$^0G_{Fe}^{liq-am} = {}^0G_{Fe}^{am} - RT\ln[1+\exp(-\Delta G_d/RT)] \quad (4)$$

where $\Delta G_d = {}^0G_{Fe}^{liq} - {}^0G_{Fe}^{am}$ is the difference between the Gibbs energy of the system when all the atoms are in the "liquid-like" state and when all the atoms are in the "solid-like" (amorphous) state, giving a continuous change of C_p from the amorphous to the liquid phase. So, Gibbs energy for pure elements ($^0G_i^{\varphi}$) is taken from the SGTE database [22] for boron, from Ref. [19] for iron.

Gibbs energy for a solution phase was modelled as:

$$G^{\varphi} = \sum_i X_i {}^0G_i^{\varphi} + RT\sum_i X_i \ln X_i + {}^{ex}G^{\varphi} \quad (5)$$

where the summation is over the components of the system.

The excess Gibbs free energy of the liquid phase has been described according to the Redlich–Kister formalism, a polynomial description popular in the CALPHAD community [23]. For the binary Fe–B system this term is then expressed as:

$$^{ex}G^{\varphi} = X_B X_{Fe} \sum_{\nu=0}^{2} {}^{\nu}L^{\varphi}(X_B - X_{Fe})^{\nu} \quad (6)$$

where $^{\nu}L^{\varphi}$ is an interaction parameter of the phase , X_{Fe} and X_B are the molar fraction of Fe and B, respectively. For the first parameter, the following temperature dependence was used [16,17]:

$$^0L^{\varphi} = A_0^{\varphi} + B_0^{\varphi}\cdot T + C_0^{\varphi}\cdot T^{-1} \quad (7)$$

whereas other interactions parameters ($^1L^{\varphi}$ and $^2L^{\varphi}$) were chosen to be temperature-independent.

The C_0^{φ} coefficient accounts for the short-range ordering of the undercooled liquid, giving a T^{-2} dependence of the excess specific heat. The amorphous phase was modelled as the liquid one, but considering $C_0^{\varphi} = 0$ and glass transition, was considered as a second-order thermodynamic transition between the liquid and amorphous phases. This means that a nil difference between entropy, enthalpy and Gibbs energy of the amorphous and liquid phases at T_g has been set in the assessment. As a consequence, the following constraints among liquid and amorphous parameters have been forced on the optimisation process:

$$A_0^{am} = A_0^{l} + 2\cdot C_0^{l}\cdot T_g^{-1} \quad (8)$$

$$B_0^{am} = B_0^{l} - C_0^{l}\cdot T_g^{-2}. \quad (9)$$

F.c.c. and b.c.c. solid solutions were modelled as subregular solutions and the various borides (Fe_3B, Fe_2B, FeB) were described as stoichiometric compounds whose Gibbs energy is given by:

$$\Delta G^{Fe_xB_y} = x\,{}^0G_{Fe}^{\alpha} + y\,{}^0G_B^{\beta} + \Delta_f H - T\cdot\Delta_f S \quad (10)$$

where $\Delta_f H$ and $\Delta_f S$ are the enthalpy and entropy of formation, respectively, and $^0G_{Fe}^{\alpha}$ and $^0G_B^{\beta}$ are the lattice stabilities of the standard reference state for Fe and B, respectively.

Owing to the lack of data, no solubility of Fe in rhombohedral B has been considered.

3. Results and discussion

Experimental data for equilibrium phases have been taken from [10]. New data related to metastable amorphous and Fe_3B phases have also been considered in order to fully assess thermodynamic parameters of the system [17].

All thermodynamic calculations in this work have been performed using the ThermoCalc software package [24]. The PARROT module has been used to assess the system, which works by minimizing an error sum among weighted experimental and calculated quantities by a least square method.

Following the previously described modelling for various stable and metastable phases [17], the Fe–B system has been reassessed (optimised parameters are reported in the Appendix). The calculated phase diagram is reported in Fig. 1 (full line). The agreement with experimental data is good and results related to stable phases are comparable to those obtained in previous assessments. Fig. 1 also shows the calculated metastable phase diagram, obtained by removing the Fe_2B boride from the calculation. Fe_3B becomes stable at a low temperature and shows an eutectic decomposition at about 1387 K and 18 at.%B according to experimental findings [25].

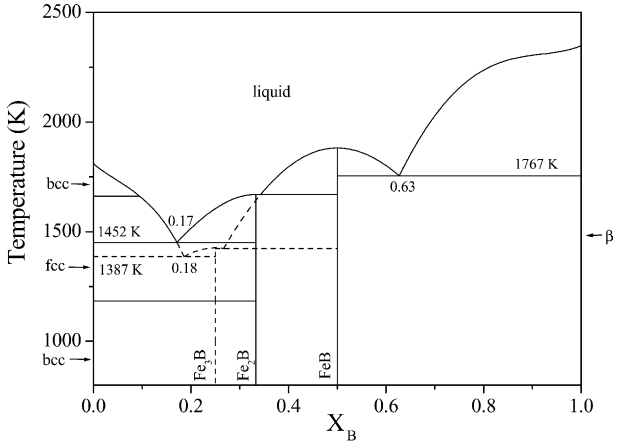

Fig. 1. Calculated Fe–B stable (continuous line) and metastable (dashed line) phase diagrams.

Fig. 2 shows a comparison among experimental and calculated crystallisation enthalpies according to various assessments. It is evident that the assessment from Ref. [10] is unable to describe experimental data. On the contrary, both assessments in this work and from Ref. [17] provide a much better description of the data, which is due to the presence of the excess specific heat term in the liquid phase [Eq. (7)].

The calculated specific heat of liquid $Fe_{83}B_{17}$ as a function of temperature is reported in Fig. 3 for different assessments. Owing to the absence of an excess specific heat, C_p values calculated from Ref. [10] are average values between specific heat of pure elements according to SGTE description [22]. Including the C_0^{φ} term in Eq. (7) for the description of undercooled liquid, a rising trend of the specific heat on undercooling is obtained, according to the experimental data available for glass forming metallic systems [26–29]. This effect may be observed in Fig. 3 for C_p values calculated from ref. [17] and from this work. A specific heat difference between the undercooled liquid and the amorphous phase of about 20–25 J/mol K is calculated at T_g (800 K in the whole composition range), which is in reasonable agreement with experimental findings [16].

A slope change of C_p at 1811 K, related to the SGTE description of pure Fe, is observed for assessments reported in [10] and [17]. The use of the new description for lattice stabilities of pure Fe [19] overcomes this unphysical result, giving a more reliable description for the specific heat of liquid alloys. At a higher boron content, the calculated excess specific heat of the liquid alloy can reach particularly high values. In the absence of experimental data for the composition dependence of C_p, a maximum value of about 46 J/K mol has been calculated for the excess specific heat at 50% at. B from Ref. [17], which appears rather high. Instead, a lower value of about 36 J/mol K has been obtained according to the assessment in this work.

A comparison among driving forces calculated according to Spaepen's model [7] and CALPHAD assessments is shown in Fig. 4 for b.c.c. and Fe_2B phases in a $Fe_{85}B_{15}$ alloy. The values calculated according to Ref. [10] are always higher than those obtained in this work. This is a consequence of the new models adopted: the presence of an excess specific heat term leads to the

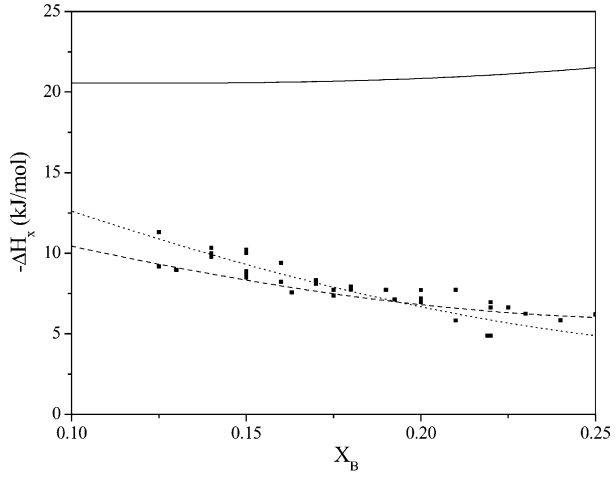

Fig. 2. Experimental and calculated crystallisation enthalpy (ΔH_x) of Fe–B amorphous alloys according to various CALPHAD assessments: full line, from Ref. [10]; dotted line, from Ref. [17]; dashed line, this work; experimental data, from Ref. [31].

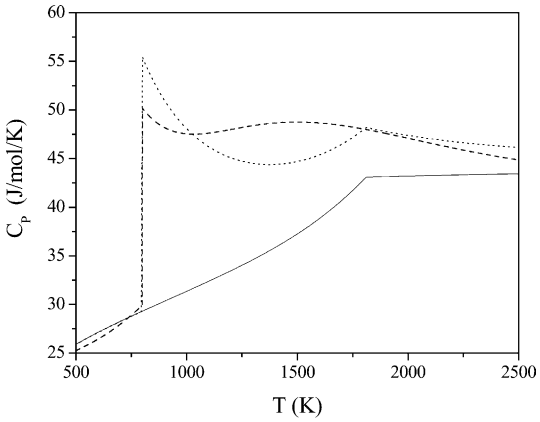

Fig. 3. Calculated specific heat (C_p) of liquid $Fe_{83}B_{17}$ as a function of temperature, according to various CALPHAD assessments: full line, from Ref. [10]; dotted line, from Ref. [17]; dashed line, this work.

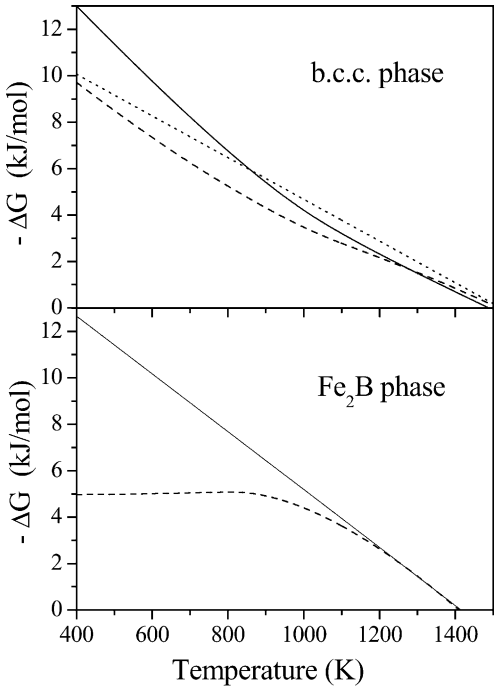

Fig. 4. Calculated driving forces for nucleation of b.c.c. solid solution and Fe_2B from liquid–amorphous $Fe_{85}B_{15}$ as a function of temperature amorphous matrix according to Eq. (3) (dotted line) and various CALPHAD assessments: full line, from Ref. [10]; dashed line, this work.

stabilisation of liquid on undercooling, so that driving forces become lower. The effect is even higher for intermetallic compounds because liquid stabilisation is stronger at intermediate compositions. Spaepen's model provides a different temperature dependence for the driving force of crystal nucleation, which is a consequence of the simple regular model used for the liquid phase.

Calculated driving forces for nucleation of different phases as a function of temperature are reported in Fig. 5 for ipoeutectic ($Fe_{85}B_{15}$) and eutetectic ($Fe_{83}B_{17}$) alloys. At low temperature, a b.c.c. solid solution has the highest driving force for both alloys, so we can estimate that this phase will nucleate first from an amorphous alloy, in agreement with experimental findings [8]. At a higher temperature, the driving force for intermetallic compounds becomes higher with respect to that for the b.c.c. phase, particularly for the eutectic alloy. It may also be observed that driving forces for Fe_3B and Fe_2B are similar, but the former is always lower than the latter. Owing to the limited solution of B in both b.c.c. and f.c.c. phases, the composition of the first nucleus (not shown) is very close to pure iron in the whole temperature and composition range.

The calculated driving forces for nucleation of different phases at 650 K, which is close to crystallisation temperature [31], are plotted in Fig. 6. It is evident that nucleation of the b.c.c. phase is preferred for low boron concentration. Nucleation of a b.c.c. solid solution is followed by boron enrichment of the amorphous matrix in the surroundings. From Gibbs energy curves at this temperature (not shown), metastable equilibrium gives a 28%B value for this amorphous matrix, which is still inside the glass forming range for this system and would then be relatively stable. In contrast, for higher concentrations (>17%B), primary Fe_2B or Fe_3B would form in metastable equilibrium with an amorphous phase containing only about 2 at.%B. This phase would then be very unstable, giving almost immediately the corresponding equilibrium b.c.c. solid solution, as observed in eutectic crystallisation. Experimental findings [25,30–32] show, in fact, that, for ipoeutectic alloys, primary crystallisation of b.c.c. almost pure Fe is followed in a second step by transformation of the remaining amorphous matrix into Fe_3B. On the contrary, for a 17 at.%B alloy an eutectic crystallisation mechanism is observed, with the simultaneous formation of b.c.c. and Fe_3B phases. For ipereutectic alloys, nucleation of primary Fe_3B ($17\% < X_B < 25\%$) and Fe_2B ($X_B > 26\%$) has been found. Fe_3B crystallises by a polymorphous mechanism from the amorphous matrix at 25%B.

As shown in Fig. 6, the driving force for Fe_3B boride is close to that of Fe_2B in the Fe-rich side, but it becomes higher at a higher boron concentration. This is in contrast to the observed crystallisation mechanism but could be due both to the accuracy of calculated quantities and the effect of interfacial energies. The confidence interval of calculated driving forces is related to the accuracy of experimental data used in the optimisation, but it is not straightforward to estimate. However a 10% value should be reasonable in this case.

On the other hand, considering the crystallisation of an amorphous $Fe_{75}B_{25}$ alloy, the nucleation frequency of Fe_3B and Fe_2B phases should be similar on the basis of the observed experimental behaviour. According to

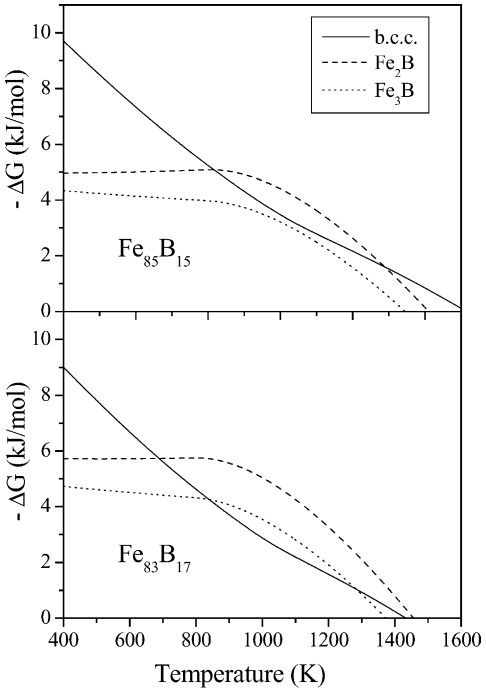

Fig. 5. Calculated driving forces for nucleation of b.c.c. solid solution, Fe_2B and Fe_3B as a function of temperature from liquid–amorphous $Fe_{85}B_{15}$ and $Fe_{83}B_{17}$.

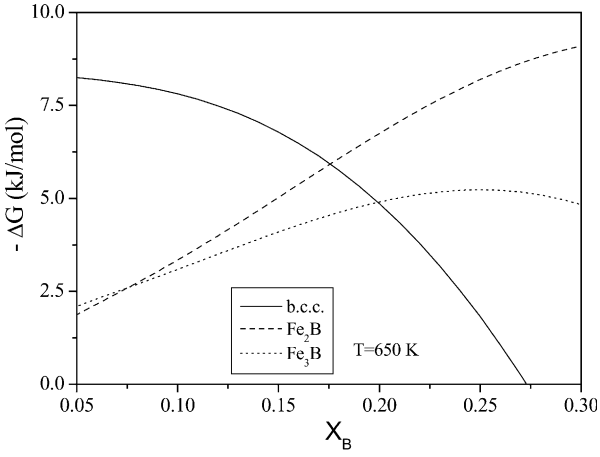

Fig. 6. Calculated driving forces for nucleation of b.c.c. solid solution, Fe_2B and Fe_3B as a function of alloy composition at $T = 650$ K.

the nucleation theory, this quantity depends on diffusivities, driving forces and interfacial energies. Diffusivities should be the same for both phases because they crystallise from the same amorphous matrix. Then, by equating the nucleation frequencies of the two phases we find

$$\left(\frac{\Delta G_{\mathrm{Fe3B,am}}}{\Delta G_{\mathrm{Fe2B,am}}}\right)^2 = \left(\frac{\gamma_{\mathrm{Fe3B,am}}}{\gamma_{\mathrm{Fe2B,am}}}\right)^3 \tag{11}$$

where $\Delta G_{\mathrm{Fe3B,am}}$, $\Delta G_{\mathrm{Fe2B,am}}$ are the nucleation driving forces of the two borides from the amorphous matrix, respectively, and $\gamma_{\mathrm{Fe3B,am}}$, $\gamma_{\mathrm{Fe2B,am}}$ are the interfacial energies between the borides and the amorphous phase.

Using calculated driving forces at 650 K we obtain a 0.64 value for the $\gamma_{\mathrm{Fe3B,am}}/\gamma_{\mathrm{Fe2B,am}}$ ratio at eutectic composition. This difference in interfacial energies, coupled with a 10% confidence interval for calculated driving forces, could explain the observed formation of the Fe_3B phase in Fe–B amorphous alloys.

4. Conclusion

The Fe–B system has been thermodynamically assessed, including amorphous and Fe_3B metastable phases. Calculated thermodynamic properties and phase diagrams are in good agreement with the available experimental data.

Driving forces for crystal nucleation have been calculated and results have been used to discuss the crystallisation behaviour. However, a complete description of the crystallisation mechanism and a quantitative evaluation of nucleation frequencies require the knowledge of interfacial energies which is not available at the moment.

Acknowledgements

Work was performed for MIUR-PRIN 2001032538 and RTN/BMG (HPRN-CT-2000-00033).

Appendix

	Lattice stabilities
Fe liquid	From [19]
Fe b.c.c., Fe f.c.c.	From [19]
B liquid, B rhombohedral	From [22] (SGTE)
B f.c.c., B b.c.c.	From [12]

Phase	Parameters
Liquid	${}^0\mathrm{L}^{\mathrm{liq}} = -59{,}360 - 6.880\,T - 4.598 \cdot 10^7 T^{-1}$
	${}^1L^{\mathrm{liq}} = 15{,}120$
	${}^2L^{\mathrm{liq}} = 46{,}060$
Amorphous	${}^0L^{\mathrm{am}} = -174{,}300 - 65.00\,T$
	${}^1L^{\mathrm{am}} = 15{,}120$
	${}^2L^{\mathrm{am}} = 46{,}060$
Fe b.c.c. (α)	${}^0L^{\alpha} = -18{,}220 + 5.477 \quad T$
Fe f.c.c. (γ)	${}^0L^{\gamma} = -47{,}630 + 32.05 \quad T$

$$G^{\varphi}_{\mathrm{ex}} = X_{\mathrm{B}} X_{\mathrm{Fe}} \sum_{\nu=0}^{2} {}^{\nu}L^{\varphi}(X_{\mathrm{B}} - X_{\mathrm{Fe}})^{\nu}$$

Redlich−Kister polynomials

Phase	Parameters
FeB	$\Delta_f H = -68{,}650$
	$\Delta_f S = -3.921$
Fe_2B	$\Delta_f H = -81{,}300$
	$\Delta_f S = -3.389$
Fe_3B	$\Delta_f H = -80{,}060$
	$\Delta_f S = -5.174$

$$\Delta G^{\mathrm{Fe}_x\mathrm{B}_y} = x\,{}^0G^{\alpha}_{\mathrm{Fe}} + y\,{}^0G^{\beta}_{\mathrm{B}} + \Delta_f H - T \cdot \Delta_f S$$

stoichiometric compounds $\mathrm{Fe_xB_y}$

References

[1] Kulik T. J Non-Crystalline Solids 2001;287:145.
[2] Greer AL. In: Dinesen AR et al., editors. Science of metastable and nanocrystalline alloys: structure, properties and modelling. Proceedings of the 22nd Ris" International Symposium on Materials Science, 2001.
[3] Coudurier L, Eustathopoulos E, Desre P, Passerone A. Acta Met 1978;26:465.
[4] Spaepen F, Fransaer J. Adv Eng Mater 2000;2(9):593.
[5] Kim WT, Cantor B. Acta Metall Mater 1994;42(9):3115.
[6] Battezzati L, Baricco M. Phil Mag 1993;B68:813.
[7] Thompson CV, Spaepen F. Acta Met 1983;31:2021.
[8] Köster U, Herold U. In: Güntherodt HJ, Beck H, editors. Glassy Metals I. Berlin: Springer-Verlag; 1981. p. 225.
[9] Van Rompaey T, Hari Kumar KC, Wollants P. J Alloys and Comp 2002;334:173.
[10] Hallemans B, Wollants P, Roos JR. Z Metallkd 1994;85:676.
[11] Okamoto H. J Phase Equilib 1995;16(4):364.
[12] Pan L, Saunders N. Presented at CALPHAD XVIII, Stockholm; 1989.
[13] Ohtani H, Hasebe M, Ishida K, Nishizawa T. Trans Iron Steel Inst Jpn 1988;28:1043.
[14] Chart TG. Comm. Comm. Eur. CECA; 1981. No 7210-CA/3/303.
[15] Kaufman L, Uhrenius B, Birnie D, Taylor K. CALPHAD 1984;8:25.

[16] Bormann R. Mater Sci Eng 1994;A178:55.
[17] Palumbo M, Bosco E, Cacciamani G, Baricco M. CALPHAD 2001;25:625.
[18] Zaitsev A, Zaitseva N, Kodentsov A. J Mater Chem 2003; 13(4):943.
[19] Chen Q, Sundman B. J Phase Equilib 2001;22:63.
[20] Christian JW. The theory of transformations in metals and alloys. 1st ed. Oxford: Pergamon Press; 1965.
[21] Ågren J, Cheynet B, Clavaguera-Mora MT, Hack K, Hertz J, Sommer F, Kattner U. CALPHAD 1995;19:449.
[22] Dinsdale AT. CALPHAD 1991;15:317.
[23] Saunders N, Miodownik AP. CALPHAD: a comprehensive guide. New York: Elsevier Science; 1998.
[24] Sundman B, Jansson B, Andersonn JO. CALPHAD 1985;9:153.
[25] Battezzati L, Antonione C, Baricco M. J Alloys Comp 1997; 247:164.
[26] Busch R. JOM- Minerals Metals and Materials Society 2000;52:39.
[27] Glade SC, Busch R, Lee DS, Johnson WL, Wunderlich RK, Fecht HJ. J Appl Phys 2000;87:7242.
[28] Fecht HJ, Wunderlich RK. Materials Science and Engineering 1994;A178:61.
[29] Lee MC, Fecht HJ, Allen JL, Perepezko JH, Ohsaka K, Johnson WL. Materials Science and Engineering 1988;97:301.
[30] Cunat C, Notin M, Hertz J, Dubois JM, Le Caer G. J Non-Cryst Solids 1983;55:45.
[31] Antonione C, Battezzati L, Cocco G, Marino F. Z Metallkd 1984;75:714.
[32] Kahn Y, Kneller E, Sostarich M. Z Metallkd 1981;72:553.